

Conformational Switching of Molecular Brushes in Response to the Energy of Interaction with the Substrate[†]

Frank Sun,[‡] Sergei S. Sheiko,^{*,‡} Martin Möller,[§] Kathryn Beers,^{||} and Krzysztof Matyjaszewski^{||}

Department of Chemistry, University of North Carolina at Chapel Hill, Chapel Hill, North Carolina 27599-3290, Institut für Technische Chemie und Makromolekulare Chemie, RWTH Aachen, D-52062 Aachen, Germany, and Center for Macromolecular Engineering, Department of Chemistry, Carnegie Mellon University, Pittsburgh, Pennsylvania 15213

Received: May 14, 2004; In Final Form: July 7, 2004

Cylindrical brush molecules adsorbed on a surface change their contour length and then switch conformation from rodlike to globular upon decrease of the surface energy of the substrate. The conformational changes result from partial desorption of poly(*n*-butyl acrylate) side chains as the surface pressure drops from 23.7 to 3.1 mN/m and the energy of interaction between the side chains and the substrate decreases from 89.7 mJ/m² to 69.1 mJ/m². At the lowest value of the interaction energy, one observes a coexistence of rodlike and globular molecules. This result is in agreement with the theoretical prediction of the rod-globule transition of surface confined brush molecules as a conformational phase transition of the first order.

Introduction

Shape responsive molecules can be designed based on the so-called molecular bottlebrushes.^{1,2} For these molecules, the conformation is largely controlled by the densely grafted side chains. In solution, steric repulsion between the side chains results in a wormlike conformation of cylindrically shaped molecules, in which the persistence length increases with the side chain length and the grafting density.^{3–7} On a surface, the conformation depends on the fraction of adsorbed side chains.^{8–10} Adsorption of side chains causes extension of the backbone due to steric repulsion of the chains, while desorption and attraction of desorbed side chains promotes a change in conformation from wormlike to globular. Adsorbed side chains reduce the systems interfacial energy by increasing the number of contacts with the surface; however, this occurs at the expense of the entropy which decreases due to extension of the side chains as well as the backbone. Recently, we have shown that this enthalpy–entropy interplay leads to a rod-globule conformational transition upon desorption of side chains caused by lateral compression of a water supported monolayer.⁸ This transition was shown to be a conformational phase transition of the first order.⁸ Additional experiments were carried out to show that this transition is purely molecular in nature, as it was also observed for single molecules.¹¹ In a previous paper, we predicted that a similar transition can occur upon decreasing the surface energy of the substrate.⁸

Here we report on the axial contraction followed by rod-globule transition of cylindrical brushes in response to the decrease in the energy of interaction between brush molecules and the underlying substrate. The interaction energy was varied by changing the substrate composition via mixing water (higher surface energy) and methanol (lower surface energy). As the interaction energy dropped from 89.7 mJ/m² on the pure water

to 69.1 mJ/m² on the 79/21 wt/wt % water/methanol mixture, brush molecules with poly(*n*-butyl acrylate) side chains demonstrated a transition from a rodlike to a globular conformation. These results support our recent studies of the rod-globule transition caused by exposing brush molecules to vapors of ethanol.¹² In the transition region, one also observes a coexistence of the globular and the rodlike conformations. The coexistence of two conformations is in agreement with the theoretical prediction of the first-order phase transition.

Experimental Section

Materials. Cylindrical brushes with poly(*n*-butyl acrylate) (PBA) side chains were prepared by the grafting of *n*-butyl acrylate (nBA) from a poly(2-(2-bromopropionyloxy)ethyl methacrylate) (pBPPEM) macroinitiator using atom transfer radical polymerization (ATRP).^{13–17} Using this synthetic technique one can prepare brush molecules with a well-defined degree of polymerization of the main chain and uniform distribution of the side chains along the backbone.^{8,18,19} In this work, we studied only one type of brushes for which the degree of polymerization of the backbone was measured to be $N = 567$ and the degree of polymerization of the side chains to be $n = 35$ (Table 1).

Characterization. Average molecular weights and molecular weight distribution were measured by gel permeation chromatography (GPC) equipped with Waters microstyragel columns (pore size 10⁵, 10⁴, 10³ Å) and three detection systems: a differential refractometer (Waters Model 410), multiangle laser light-scattering (MALLS) detector (Wyatt, DAWN EOS), and a differential viscometer (WGE Dr. Bures, η -1001). The 90° detector was calibrated using toluene. All other detectors were normalized to the 90° signal. The refractive index increment dn/dc was determined with an Otsuka Photol RM-102 differential refractometer. Static light scattering (SLS) measurements were done using a Brookhaven Goniometer equipped with a Coherent argon laser using the 514 nm line, an operating power of 20–100 mW, and an angle range of 15–155°. Solutions were made with a concentration range from 10⁻⁴ to

[†] Part of the special issue "Tomas Baer Festschrift".

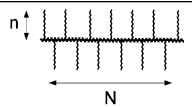
^{*} Corresponding author e-mail: sergei@email.unc.edu.

[‡] University of North Carolina at Chapel Hill.

[§] Institut für Technische Chemie und Makromolekulare Chemie.

^{||} Carnegie Mellon University.

TABLE 1: Molecular Characteristics of PBA Brush Molecules

	$m_n^a \times 10^6$	$N^{b)}$	$M_n^c \times 10^6$	$M_n^d \times 10^6$	n_n^e
	0.15	567±35	2.7±0.15	2.5±0.22	35±3

^a Number average molecular weight of the macroinitiator (backbone). ^b Number average degree of polymerization of the backbone $N = m_n/m_0$, where $m_0 = 265$ – molecular weight of BPEM monomeric unit. ^c Number average molecular weight determined by MALLS-GPC, $dn/dc = 0.068$. ^d Number average molecular weight determined by the AFM-LB method. ^e The number average degree of polymerization of the side chains was determined as $n_n = (M_n - m_n)/N_n M_0$, where M_n – number average molecular weight of the PBA brush measured by MALLS-GPC, m_n = number average molecular weight of the main chain determined by MALLS-GPC of the macroinitiator, and $M_0 = 128$ – molecular weight of BA monomeric unit.

10^{-2} g/mL in THF that had been filtered using $0.2 \mu\text{m}$ NALGENE PTFE filters.

Sample Preparation. Monolayers of brush molecules were prepared by the Langmuir–Blodgett technique using a KSV-5000 instrument filled with double-distilled water (Milli-Q). Compressed monolayers were transferred onto a mica substrate at 25°C and a transfer speed of 1.0 mm/min . During transfer, the pressure was kept constant. A transfer ratio of 0.98 was determined separately by using a larger substrate at the same transfer speed. A value close to unity indicates that the transfer did not cause significant changes in the mass density of the water-supported monolayer.

Measurements. AFM images were collected using a Multimode Atomic Force Microscope (Veeco Metrology Group) equipped with a Nanoscope IIIa control station in tapping mode. We used Si cantilevers (Mikromasch-USA) with a resonance frequency of about 140 kHz and a spring constant of about 5 N/m . The radius of the probe was less than 10 nm . To ensure accurate counting of visualized molecules, several images were collected from the same sample but in different areas, using different scan sizes and scan directions. For every sample an average of 300 molecules was counted. The counting was performed using a custom software program for analysis of digital images. The program identifies the molecular contour and determines the contour length, the end-to-end distance, and the curvature distribution.

Results and Discussion

To create a change in the interaction energy between PBA brushes and the subphase used in the Langmuir–Blodgett technique, methanol was mixed into the traditional water subphase. Methanol was chosen because of its low surface energy ($\gamma = 23 \text{ mN/m}$ at 25°C) and because it is completely miscible with water ($\gamma = 72 \text{ mN/m}$ at 25°C). By increasing the percentage of methanol in the water subphase the interaction energy as well as the surface tension of the mixture decreased. The mixtures along with the corresponding surface and interaction energies are depicted in Table 2.

The Langmuir–Blodgett experiments were all run under the same experimental conditions except for variations in the subphase. The surface pressure-molecular area isotherms from those experiments are shown in Figure 1. The isotherms all have the same main features in that each has two distinct plateaus that occur at the same critical molecular areas. The only difference between the curves is the location of the pressure onset and the maximum pressure achieved. In fact, the curves obtained on water/methanol mixtures can be collapsed onto the water curve by shifting the curves along the π -axis.

The difference in the curves can be clearly seen that with changing surface energy one gets a decrease in the overall surface pressure $\pi = \gamma_s - \gamma_f$, where γ_s and γ_f are the surface energies of the subphase and the free energy of the film (per unit area), respectively. For thick films, i.e., at large degrees of

TABLE 2: Surface Tensions and Interaction Energies of Varying Mixtures of Methanol and Water

percentage of methanol	γ_s^a , mN/m	γ_s^p , mN/m	ϕ^c	π^d , mN/m	W_{sl}^e , mJ/m ²	W_{sl}^p , mJ/m ²	ϕ^g
0	70.3	50	0	23.7	89.7	38	0
5	60.8	40	0.20	15.9	81.9	31	0.19
10	55.3	35	0.30	11.2	77.2	26	0.32
15	51.1	31	0.38	6.8	72.8	21	0.45
20	48.8	28	0.42	3.9	69.9	19	0.50
21	47.2	27	0.46	3.1	69.1	18	0.53
22	46.7	26	0.47	2.7	68.7	17	0.55

^a Surface tension of the subphase according to percentage of methanol in water ($\pm 0.2 \text{ mN/m}$). ^b Contribution of dipole–dipole interactions to the surface tension of the subphase $\gamma_s^p \cong \gamma_s - \gamma_s^d$, where $\gamma_s^d = 20 \pm 2 \text{ mN/m}$ is the contribution of dispersion forces. ^c The fraction of methanol at the free surface of the subphase was calculated as $\phi \cong 1 - \gamma_s^p/\gamma_{water}^p$, where $\gamma_{water}^p = 50 \pm 2 \text{ mN/m}$ is the contribution of polar interactions in pure water. ^d Surface pressure from the isotherms measured at high compressions, i.e., for thick films (Figure 1). ^e The interaction energy (or work of adhesion) $W_{sl} = \pi + 2\gamma_l$ was determined for thick PBA films at large compressions, using $\gamma_l = 33 \text{ mN/m}$ —the surface tension of PBA and π —the surface pressure measured for thick films at high degrees of compression. ^f Contribution of polar interactions to the interaction energy $W_{sl}^p \cong W_{sl} - W_{sl}^d$, where $W_{sl}^d \cong 2\sqrt{\gamma_s^d \cdot \gamma_l^d}$ is the contribution of dispersion forces and $\gamma_l^d \cong \gamma_l = 33 \text{ mN/m}$ —surface tension of PBA at 25°C . ^g The fraction of methanol at the free surface was calculated as $\phi \cong 1 - W_{sl}^p/W_{water}^p$, where $W_{water}^p \cong 38 \text{ mJ/m}^2$ is the contribution of polar (nondispersion) interactions between PBA and water molecules.

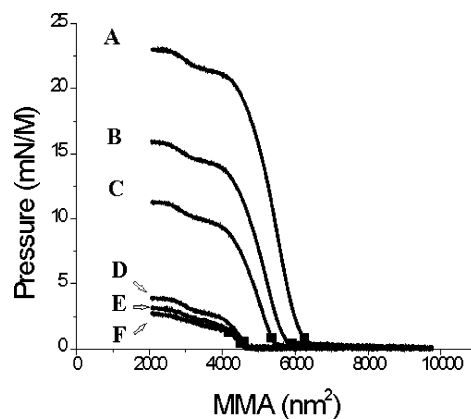


Figure 1. Compression-expansion isotherm for PBA brushes at different percentages of methanol mixed in water: A-0% (no methanol), B-5%, C-10%, D-20%, E-21%, F-22%. Squares (■) on the isotherms show the area per molecule and pressure at transfer. Decreasing the surface energy has a profound affect on the maximum pressure achieved during compression.

compression, the free energy of the film is mainly determined by the surface energy of the film and the interfacial energy, i.e., one can write $\gamma_f \cong \gamma_l + \gamma_{sl}$, where γ_l is the surface energy of the poly(*n*-butyl acrylate) film (liquid at room temperature) and γ_{sl} is the interfacial energy at the film-subphase interface. One can also determine the interaction energy or the work of

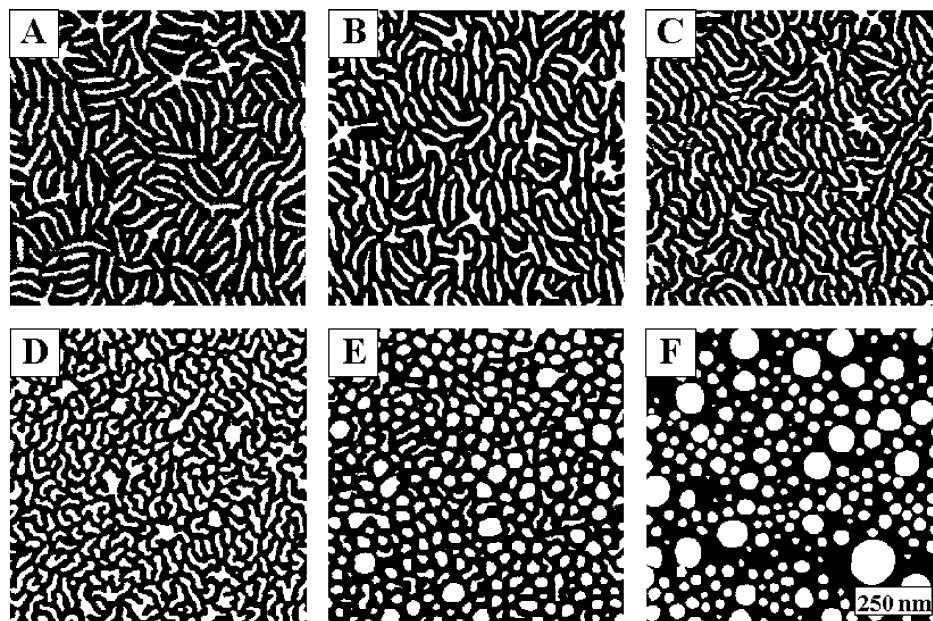


Figure 2. AFM micrographs (cropped from $2 \times 2 \mu\text{m}^2$ images) of monolayers of PBA brushes transferred on mica at different percentages of methanol in water: A-0% (no methanol), B-5%, C-10%, D-20%, E-21%, F-22%. One can see the obvious change in conformation as the fraction of methanol is increased. Multiple images of each sample were analyzed to obtain molecular dimensions of the PBA brushes.

adhesion between PBA and a water/methanol substrate as $W_{sl} = \pi + 2\gamma_l$. Table 2 summarizes the surface tensions γ_s and the interaction energies W_{sl} calculated for different subphases at large compressions where the surface pressure levels off. Both the surface tension and the interaction energy reduce with larger fraction of methanol. This indicates that the interaction between the PBA film and the water/methanol subphase is largely determined by the strong dipole–dipole interactions between the polar acrylate units and water molecules. The number of acrylate/water contacts decreases upon addition of methanol to the subphase.

In the first approximation assuming that contributions of different types of interactions are additive, the interaction energy is a sum of dispersion forces and nondispersion (polar and hydrogen bonding) interactions, i.e. $W_{sl} = W_{sl}^d + W_{sl}^p$. The dispersion contribution can be calculated as $W_{sl}^d \cong 2\sqrt{\gamma_s^d \gamma_l^d}$, where γ_s^d and γ_l^d are the dispersion force contributions of the surface tensions of the water/methanol subphase and the PBA liquid, respectively. Using literature data $\gamma_s^d = 20 \pm 2$ mN/m for water/methanol and $\gamma_l^d \cong 33$ mN/m for PBA, one can calculate the contribution of nondispersion (polar and H-bonding) interactions in excess of dispersion force interactions as $W_{sl}^p \cong W_{sl} - 2\sqrt{\gamma_s^d \gamma_l^d}$. In the same way, one can also calculate the contribution of polar interactions to the surface tension of the water/methanol subphase, i.e. $\gamma_s^p \cong \gamma_s - \gamma_s^d$, where $\gamma_s^d = 20 \pm 2$ mN/m is the contribution of dispersion forces. The obtained values are summarized in Table 2. Note that both the γ_s^p and W_{sl}^p decrease with the fraction of methanol in a similar fashion. From these data, one can roughly estimate the fraction of methanol molecules at the free surface of the subphase which differs from the percentage of methanol in bulk solution (Table 2). The addition of methanol results in depletion of water molecules at the free surface. This corroborates our conclusion that nondispersion interactions between PBA side chains and water molecules dominate the interfacial interactions in these systems.

The first plateau region is of greatest interest in this experiment because it is the location of the rod-globule transition.⁸ Thus in the experiment different subphases with

TABLE 3: AFM Data on Molecular Dimensions of PBA Brushes Deposited on a Surface of Varying Mixtures of Methanol and Water

fraction of methanol	D_s^a , nm	L_n^b , nm	PDI ^c	A_{AFM}^d , nm ²	A_T^e , nm ²	l_m^g , nm
0	51 ± 2.0	128	1.13	6595	6249	0.23
5	47 ± 2.0	122	1.15	6009	5906	0.22
10	44 ± 2.3	114	1.16	5382	5344	0.20
15	43 ± 3.1	111	1.19	5116	5194	0.19
20	44.5 ± 1.4	96	1.15	4480	4602	0.17
21	44 ± 4.8	82	1.07	4140	4495	0.14
22	N/A ^f	N/A ^f	N/A ^f	4100	4179	N/A ^f

^a Number average distance between brush molecules. ^b Number average contour length of brush molecules. ^c Length polydispersity index $\text{PDI} = L_w/L_n$ of brush molecules. ^d Number average area per brush molecule (± 200 nm²). ^e Number average area per brush molecule measured during the LB transfer. ^f The values could not be determined due to coalescence of molecules. ^g Contour length per monomeric unit $l_m = L_n/N$.

different fractions of methanol were examined until the phase transition region occurred. For each different subphase, a monolayer of PBA brush molecules was transferred on mica at a low pressure of about 0.5 mN/m. The LB monolayers were examined by AFM. The AFM technique was vital to this experiment as it allowed visualization of the changes in individual molecules because of variation of surface energy. Figure 2 shows a series of AFM micrographs obtained for different fractions of methanol in water. The white threads in the images correspond to the backbone, whereas extended side chains cover the areas between the threads. As the fraction of methanol is increased, the molecules change their conformation.

One can discriminate two types of conformational changes. First, the average contour length of the brush molecules decreases. Second, at a certain fraction of methanol the rodlike molecules undergo a transition to a globular conformation. While it is hard to see from the figure, the distance between molecules does not change significantly before collapse into a globule. The intermolecular distances and the lengths of brush molecules can be independently measured by AFM. The obtained results are summarized in Table 3 and plotted in Figure 3 which shows variations in the length and the distance between molecules upon

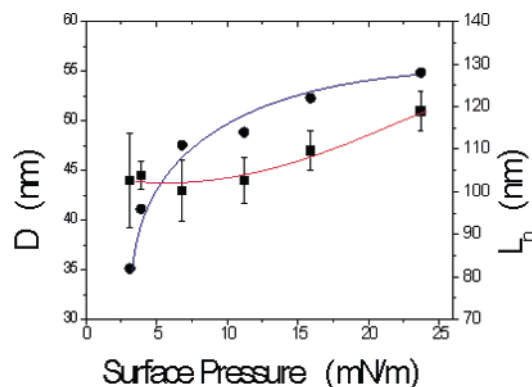


Figure 3. Variation of molecular dimensions of the polymer brushes as a function of surface pressure: (■) distance between backbones D and (●) number of average contour length L_n . The lines on the figure are only to show the trend in the data and have no quantitative meaning. The plots show that the average length of the molecules decreases, but the distance between molecules virtually remains the same at different surface pressures.

adding methanol to the water subphase. The lines in the figure are only there to guide the reader and to show that there is a small decrease in the distance as methanol is added to the subphase, while the length changes significantly. After the initial decrease in the distance, it nearly remains constant at 44 nm after more methanol is introduced into the subphase. The length of brush molecules demonstrates an opposite behavior. The length decreases only slightly at small fractions of methanol, while it drops significantly when more methanol is added into the water subphase. In total, the length shrinks by a factor of 1.5 as the surface pressure decreases from 23.7 to 3.1 mN/m. Note that on pure water the molecular backbone is almost fully extended, since the length per monomeric unit $l_m = L_n/N_n$ is equal to 0.23 ± 0.02 nm (Table 3), which is close to the length $l_0 \cong 0.24$ nm of a monomeric unit in an all-trans polymer chain. The observed length variation is in agreement with theory. As the energy of interaction with the substrate is decreased the number of side chains that detach from the surface and collapse onto the backbone becomes greater. With less side chains in contact with the surface, the backbone is no longer forced into extension but can relax and more curvature can be seen as in Figure 2D. The area per molecules was also determined by AFM and is solely dependent upon the length of the molecules, as the distance between molecules remains constant (Table 3). These rodlike molecules could thus be thought of as molecular springs or actuators whose length is sensitive not only to changes in pressure but also to the surface energy of the material that they are on.

Qualitative changes in conformation were observed as the surface pressure of the film decreased to 3.1 mN/m and the interaction energy decreased to 69.1 mJ/m² for a mixture of 21% methanol in water. At this value of the interaction energy, poly(*n*-butyl acrylate) brushes demonstrate a transition from a rodlike to a globular conformation. Moreover, Figure 2E shows a coexistence of two conformations, i.e., rods and globules at the same temperature and the same surface pressure. The coexistence can be demonstrated by constructing a histogram of the length distributions for different fractions of methanol as seen in the AFM micrographs (Figure 4). One can see that with increasing percentages of methanol the histogram shifts further to the left because of decreasing average length. However at 21%, the size distribution reveals two peaks corresponding to the two different species. The peaks are blurred together because the difference in linear dimensions between the rods and globules in the transition region is small.

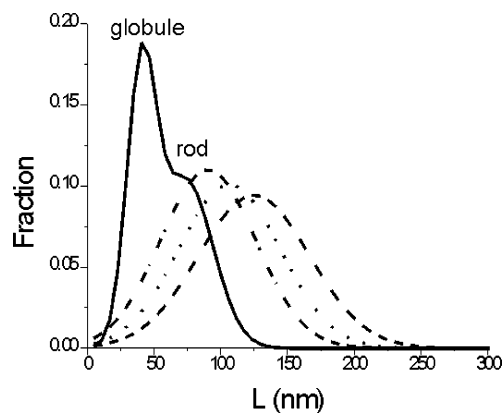


Figure 4. Histograms of the length distribution measured by AFM: water (---), 10% (---), 20% (---), 21% (—). The length distribution shifts to the left and becomes narrower as the fraction of methanol is increased. At 21% there are two separate peaks showing the coexistence of the rod and globule phases.

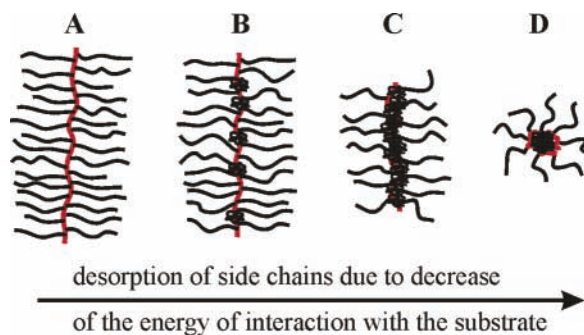


Figure 5. Illustration of the rod-globule transition upon decreasing the interaction energy: (A) side chains are adsorbed to the surface and backbone is extended, (B) side chains begin to detach and collapse on the backbone; those side chains that remain adsorbed on substrate get more space to coil and reduce their extension, (C) further desorption of side chains allows the backbone to contract from its extended state, and (D) aggregation of desorbed side chains causes the molecule to go from rodlike to globular.

In the next mixture observed all of the rods have completely collapsed into globules at 22% methanol in water. Thus the rod-globular transition is very sensitive to the surface energy of the subphase. One can see in Figure 2F, the small globules and much larger ones that form when small globules coalesce together. Further samples show even greater coalescence of molecules into larger globules.

The following illustration (Figure 5) depicts the pathway for the conformational changes for the rod-globule transition. In Figure 5A, the side chains of the molecule are adsorbed on the water subphase where the adsorbed side chains cause extension of the backbone. As described earlier the adsorbed side chains reduce the systems interfacial energy by increasing the contacts with the surface. Upon decrease of the interaction energy by the addition of methanol as depicted in Figure 5B some of the side chains detach from the surface and coil up upon the backbone. As some side chains leave the surface, other side chains that remain adsorbed on the substrate begin to coil to gain back some of the entropy lost by extension. At this stage the backbone remains extended showing only weak changes in the average contour length of brush molecules. As the PBA/water interaction is further decreased by addition of more methanol, more side chains detach from the surface, but the distance between molecules remains constant because the backbone starts to contract as depicted in Figure 5C. The contraction is also favored by attraction and aggregation of

desorbed side chains. Note that on this stage the molecules remain rodlike since their conformation is stabilized by those side chains that remain adsorbed on the substrate. Finally, as shown in Figure 5D, by further increasing the methanol fraction, the rod-globule transition occurs in which the desorbed side chains aggregate into a globule, while the desorbed side chains form a circular corona around.

Conclusion

Cylindrical brush molecules do indeed switch conformations from rodlike to globular upon decrease of the surface energy of the substrate. These types of molecules can serve a dual purpose as they can act as pressure sensors but also react in response to changes in the surface energy of a substrate they are spread upon. AFM measurements allowed for the observations of these conformational changes. By AFM, we were able to observe the coexistence of the rodlike and globular molecules. Thus agreeing with the theory that the coexistence of two conformations indicates that the rod-globule transition of surface confined brush molecules is a phase transition of the first order.

Acknowledgment. This work was financially supported by the NSF grants ECS 01-03307 and DMR 0306787 and CRP Consortium at CMU.

References and Notes

- (1) Sheiko, S. S.; Moeller, M. *Chem. Rev.* **2001**, *101*, 4099.
- (2) Li, C.; Gunari, N.; Fischer, K.; Janshoff, A.; Schmidt, M. *Angew. Chem., Int. Ed.* **2004**, *43*, 1101–1104.
- (3) Birshtein, T. M.; Borisov, O. V.; Zhulina, E. B.; Khokhlov, A. R.; Yurasova, T. A. *Polym. Sci. USSR* **1987**, *29*, 1293–1300.
- (4) Fredrickson, G. *Macromolecules* **1993**, *26*, 2825–2831.
- (5) Subbotin, A.; Saariaho, M.; Ikkala, O.; ten Brinke, G. *Macromolecules* **2000**, *33*, 3447–3452.
- (6) Terao, K.; Nakamura, Y.; Norisuye, T. *Macromolecules* **1999**, *32*, 711–716.
- (7) Gerle, M.; Fischer, K.; Schmidt, M.; Roos, S.; Müller, A. H. E.; Sheiko, S. S.; Prokhorova, S. A.; Möller, M. *Macromolecules* **1999**, *32*, 2629–2637.
- (8) Sheiko, S. S.; Prokhorova, S. A.; Beers, K. L.; Matyjaszewski, K.; Potemkin, I. I.; Khokhlov, A. R.; Moller, M. *Macromolecules* **2001**, *34*, 8354.
- (9) Stepanyan, R.; Subbotin, A.; ten Brinke, G. *Phys. Rev. E* **2001**, *63*, 061805.
- (10) Potemkin, I. I.; Khokhlov, A. R.; Sheiko, S. S.; Prokhorova, S. A.; Beers, K.; Matyjaszewski, K. *Macromolecules* **2004**, *37*, 3918–3923.
- (11) Lord, S. J.; Sheiko, S. S.; LaRue, I.; Lee, H.; Matyjaszewski, K.; *Macromolecules* **2004**, *37*, 4235–4240.
- (12) Gallyamov, M. O.; Tartsch, B.; Khokhlov, A. R.; Sheiko, S. S.; Börner, H. G.; Matyjaszewski, K.; Möller, M. *Chem.-Eur. J.* **2004**, in press.
- (13) Wang, J.-S.; Matyjaszewski, K. *J. Am. Chem. Soc.* **1995**, *117*, 5614–5615.
- (14) Patten, T. E.; Xia, J.; Abernathy, T.; Matyjaszewski, K. *Science* **1996**, *272*, 866–868.
- (15) Patten, T. E.; Matyjaszewski, K. *Adv. Mater.* **1998**, *10*, 901–915.
- (16) Matyjaszewski, K.; Xia, J. *Chem. Rev.* **2001**, *101*, 2921–2990.
- (17) Davis, K. A.; Matyjaszewski, K. *Adv. Polym. Sci.* **2002**, *159*, 2–166.
- (18) Beers, K. L.; Gaynor, S. G.; Matyjaszewski, K.; Sheiko, S. S.; Moeller, M. *Macromolecules* **1998**, *31*, 9413.
- (19) Boerner, H. G.; Beers, K. L.; Matyjaszewski, K.; Sheiko, S. S.; Moeller, M. *Macromolecules* **2001**, *34*, 4375.